AIP | The Journal of Chemical Physics

# Hybrid chromophore/template nanostructures: A customizable platform material for solar energy storage and conversion

Alexie M. Kolpak and Jeffrey C. Grossman

Citation: The Journal of Chemical Physics **138**, 034303 (2013); doi: 10.1063/1.4773306
View online: http://dx.doi.org/10.1063/1.4773306
View Table of Contents: http://scitation.aip.org/content/aip/journal/jcp/138/3?ver=pdfcov
Published by the AIP Publishing



# Hybrid chromophore/template nanostructures: A customizable platform material for solar energy storage and conversion

Alexie M. Kolpak and Jeffrey C. Grossman
*Department of Materials Science and Engineering, Massachusetts Institute of Technology, Cambridge, Massachusetts 02139, USA*

(Received 8 November 2012; accepted 4 December 2012; published online 15 January 2013)

Challenges with cost, cyclability, and/or low energy density have largely prevented the development of solar thermal fuels, a potentially attractive alternative energy technology based on molecules that can capture and store solar energy as latent heat in a closed cycle. In this paper, we present a set of novel hybrid photoisomer/template solar thermal fuels that can potentially circumvent these challenges. Using first-principles computations, we demonstrate that these fuels, composed of organic photoisomers bound to inexpensive carbon-based templates, can reversibly store solar energy at densities comparable to Li-ion batteries. Furthermore, we show that variation of the template material in combination with the photoisomer can be used to optimize many of the key performance metrics of the fuel—i.e., the energy density, the storage lifetime, the temperature of the output heat, and the efficiency of the solar-to-heat conversion. Our work suggests that the solar thermal fuels concept can be translated into a practical and highly customizable energy storage and conversion technology.
 [http://dx.doi.org/10.1063/1.4773306]

Reversibly storing solar energy in the conformation of molecular photoisomers—known as solar thermal fuels (STFs)—and releasing it as heat in a controlled manner is a promising alternative renewable energy concept. Translating this concept into a practical large-scale technology, however, will require the development of new solar thermal fuels that overcome the technical challenges that beset many of the candidate molecules studied in the past: low energy density; short storage lifetime; low quantum yield; small overlap with the solar spectrum; irreversible degradation upon repeated cycling; and/or high cost.

Previous investigations of STFs have primarily focused on three classes: Norbornadiene/quadricyclane derivatives, which have a relatively high energy density, but suffer from degradation;[1,2] (Fulvalene)tetracarbonyldiruthenium (RuFv) derivatives,[3–5] which do not degrade, but have significantly lower energy densities, as well as restricted utility due to dependence on expensive Ru metal; and azobenzenes, which are of great interest for numerous applications[6–13] due to their low cost and highly cyclability, among other properties, but typically make poor energy storage molecules[14,15] due to low energy density and/or short storage lifetime. In addition, many of the molecules in all three classes absorb in the UV and/or exhibit a low quantum yield for photoisomerization to the metastable state, and consequently can store only a limited fraction of the solar irradiance. Efforts to improve the properties of these molecules have had mixed success, with increased quantum yield or overlap with the solar spectrum often coming at the price of a decrease in the stored energy and/or the storage lifetime.[2,16,17]

Recently we theoretically demonstrated that chemically linking azobenzene photoisomers to carbon nanotube (CNT) templates to form highly ordered, close-packed arrays enables one to decouple and increase both the energy density and the storage lifetime of azobenzenes by designing specific chemical interactions between neighboring molecules.[19] While the specific azo/CNT system shows promise—and is useful in terms of demonstrating a concept—it is imperative to understand whether that concept is limited to the azo/CNT system or can be more broadly applied. Furthermore, understanding whether the concept can be extended to control other key properties, such as photoabsorption is also essential, as it could provide a highly tunable platform for developing STFs with properties specifically designed to meet the varying metrics of different applications.

In this paper, we address these and other questions. Using first-principles density functional theory (DFT), we demonstrate that a range of inexpensive carbon-based materials can serve as templates to induce artificial ordered phases in azobenzene derivatives and thereby modify not only the energy density and storage lifetime, but also the electronic and optical properties, the chemical and thermal stability, and the temperature at which heat is released when the thermal back reaction is triggered. Although we focus on azobenzene-based photoisomers and carbon-based templates in this study, our results strongly suggest that one can employ the same principles to design effective STFs composed of combinations of many different photoisomer and template materials. Our work, therefore, opens up an enormous phase space for the design of STFs, and also provides guidelines for optimizing them to meet the differing metrics required for different applications, thereby providing a platform for the development of customizable and economical STFs.

We use DFT computations, as described in the supplementary material,[18] to examine the behavior of two general classes of azobenzene derivatives bound to the six different template materials illustrated in Fig. 1. Molecules in class I, such as **1b** in the figure, are based on the results of our

 

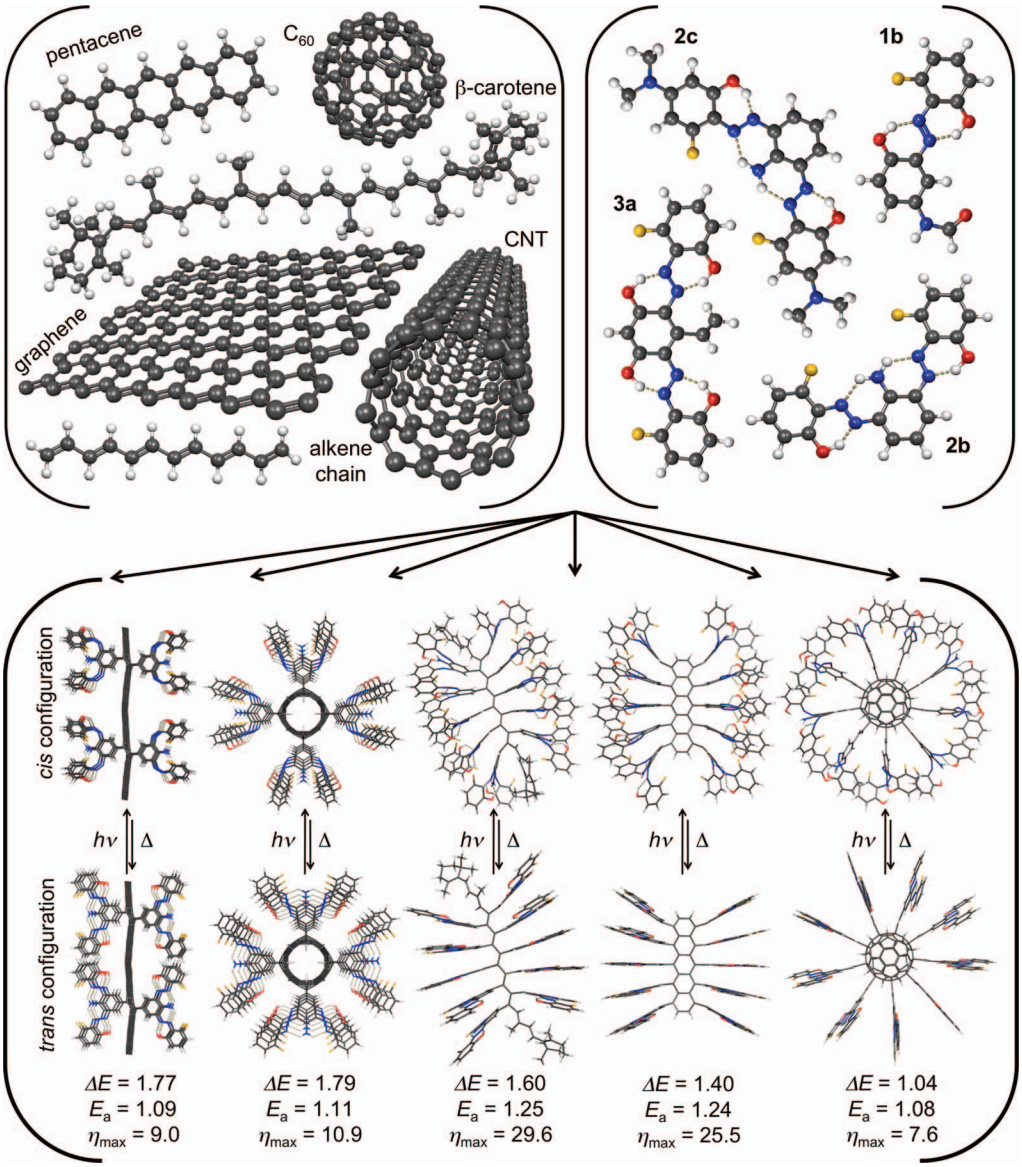


FIG. 1. (Top) The template materials and several of the azo derivatives considered in this study, which together make up only a small segment of the enormous phase space spanned by the photoisomer/template STF platform concept. (Bottom) Computed atomic structure and properties of, from left to right: **2b**/graphene, **2b**/CNT, **2b**/$\beta$-carotene, **2b**/pentacene, and **2b**/$C_{60}$. White, dark gray, blue, red, and orange balls/sticks represent H, C, N, O, and F atoms, respectively.

previous work,[19] in which *ortho* substituents were demonstrated to be effective for tuning both energy storage and thermal stability in azobenzene/CNT systems. These molecules are also of practical interest as CNTs have been functionalized with similar azo derivatives and successful photoswitching has been experimentally demonstrated in the resulting nanostructures.[12,13]

The second class of azobenzene derivatives (class II) are formed by adding a (phenylazo-) derivative to azobenzene to make 1,3-bis(phenylazo)benzenes, such as molecule **2b,** shown in the upper right panel of Fig. 1. These molecules each contain two azo groups, potentially doubling the amount of stored energy with only a 33% increase in molecular weight and volume and significantly increasing the energy density. The class II derivatives are covalently bound to the templates at the phenyl carbon either *meta* or *ortho* to the two azo groups, resulting in two different molecular geometries, as illustrated by molecules **2b** and **3b**, respectively, in Fig. 1. All azo derivatives considered in this study are illustrated in Fig. S1 in the supplementary material.[18]

To be considered a "good" template for STFs, a material must satisfy a number of important criteria. For most applications, it should be light weight and low volume; composed of cheap and abundant elements; transparent over the range of wavelengths absorbed by the photoisomer; and thermally stable with respect to degradation at temperatures greater than $T_{release}$, the temperature of the heat that is released upon triggering the STF. In addition to exhibiting these materials properties, a good template must also facilitate tuning of the energetic, electronic, and optical properties of the photoisomer/template hybrids in order to optimize the key parameters that govern practical use: energy storage density, storage lifetime, temperature of the released heat, and efficiency of the solar-to-heat conversion.

In terms of fundamental physical properties that we can compute, this optimization can be pursued via three routes:

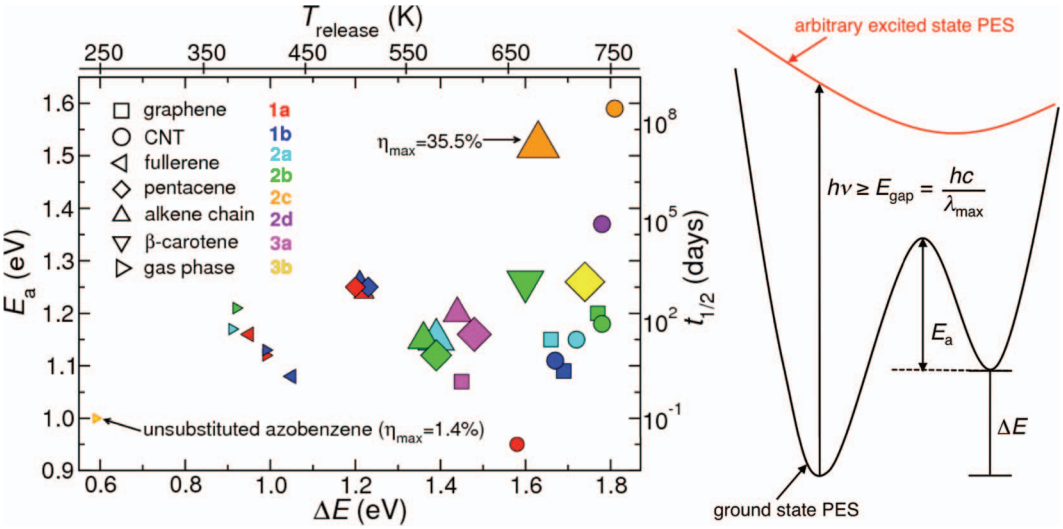


FIG. 2. (Left) Computed thermal activation barrier ($E_a$) vs stored energy per molecule ($\Delta E$) for the photoisomer/template hybrids and gas phase azo derivatives in this study. The storage lifetime ($t_{1/2}$) and the temperature of the released heat ($T_{release}$), estimated from $E_a$ and $\Delta E$, respectively, are indicated by the alternate axes. Symbols are scaled to illustrate relative values of $\eta_{max}$, the maximum external efficiency. All data are also reported in the supplementary material.[18]

First, the energy stored per photoisomer, $\Delta E$, can be increased in order to increase both $T_{release}$ and the volumetric and gravimetric energy densities (assuming constraints on volume and weight are met). Second, the barrier to the thermal back reaction, $E_a$, can be tuned to give a half-life of the metastable state, $t_{1/2}$, in the desired range; alternatively, $E_a$ can be tuned to enable thermal triggering of the heat release within a specific temperature range. Finally, the HOMO-LUMO gap, $E_{gap}$, can be decreased such that the overlap with the solar spectrum, and thus the external efficiency, $\eta$, of the solar-to-heat conversion, is maximized. Below, we identify the general atomic-scale structural and electronic properties that make a template effective at tuning each of these fundamental properties.

The data in Fig. 2 demonstrate that the key fundamental properties of a given photoisomer are not immutable, but can be tuned over a large range by introducing templates with various geometries and electronic properties. For example, the value of $\Delta E$ ranges over ≈0.5 eV/azo for molecules **1b** and **2b** across the various templates, which translates into a change of ∼200 K in $T_{release}$; including the gas phase values, the range of $\Delta E$ is doubled so that, for example, $350 < T_{release} < 750$ for molecule **2b**. Similarly, the figure shows that $E_a$ varies between 1.1 and 1.25 eV/azo for **1b** and **2b**, leading to a range of storage lifetimes spanning three orders of magnitude; other molecules exhibit the same or larger ranges in lifetime as a function of template identity. The external efficiency, which depends on both $\Delta E$ and the HOMO-LUMO gap, also exhibits highly template-dependent behavior, varying from a little over 1% for non-templated azobenzene up to 30%–35% for several photoisomer/template hybrids. Below, we discuss the origins of the observed variation for each of these properties.

Figure 2 shows that CNT and graphene templates generally lead to large values of $\Delta E$ (>∼1.6 eV/azo for most of the molecules). In comparison, the molecular templates pentacene and dodecene tend to enable smaller increases in $\Delta E$ compared to gas phase molecules. However, there are important counter-examples to these trends: molecules on the $\beta$-carotene molecular template exhibit large values of $\Delta E$ similar to those on CNT and graphene templates, while molecules on fullerene templates show little change in $\Delta E$ with respect to gas phase molecules; in addition, the **3b**/pentacene and **2c**/dodecene systems have significantly larger $\Delta E$ values than the other systems with pentacene and dodecene templates. To describe these results, and to enable prediction of template-induced changes in $\Delta E$, it is useful to classify the photoisomer/templates systems based on their ability to constrain the molecular degrees of freedom of the bound photoisomers—or, considered another way, the resistance of the template to photoisomer-induced deformation. This rigidity plays a key role in determining both the dominant type and strength of interactions between neighboring photoisomers, and thus the energy storage capacity and lifetime of the hybrid STF.

The variation in $\Delta E$ with photoisomer/template rigidity can be seen clearly in Fig. 1, which depicts the optimized atomic structures for the fully cis and fully trans configurations of the **2b**/template hybrids. In general, as the figure illustrates, bound photoisomers form a highly ordered close-packed two-dimensional array on the planar graphene template. As a result of this packing, rotations of the photoisomers are highly constrained by interactions with neighboring molecules or with the graphene itself. Since the extended nature of the graphene does not enable sufficiently large local template deformation to relax these constraints, the bound photoisomers are forced to adopt a highly strained configuration in the non-planar cis state, leading to large values of $\Delta E$. Similarly, the photoisomers on a CNT template are sterically prevented from rotation by the presence of close-packed neighbors along the nanotube axis. In contrast, the molecular templates can deform significantly, rotating around the plane of the template to accommodate the strain induced by the bound photoisomers. In addition, due to the much shorter length of the template along the packing direction, the photoisomers can fan out in the plane of the template to adopt a less strained cis configuration. This is taken to an extreme in

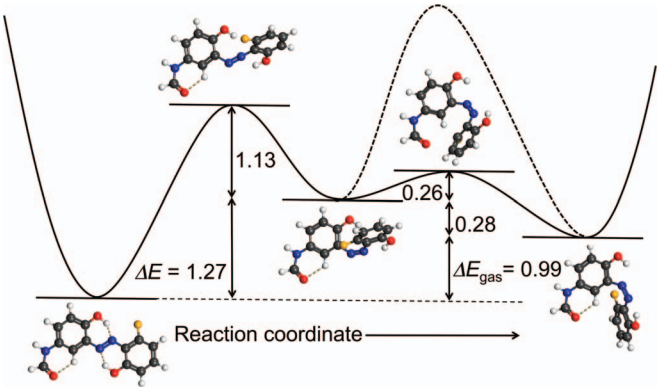


FIG. 3. The transition pathway and thermal isomerization barriers for molecule **1b** in the gas phase (solid black curve). On a template, steric interactions impose a very large barrier (dashed black curve) that prevents the cis-to-cis isomerization, kinetically trapping the higher energy cis isomer (center) and storing energy $\Delta E$, an amount larger than that stored in the gas phase ($\Delta E_{\text{gas}}$). White, dark gray, blue, red, and orange balls are H, C, N, O, and F atoms. Dashed gold lines represent H-bonds.

photoisomer/fullerene hybrids, in which the bound photoisomers behave similar to gas phase molecules due to the high curvature of the template in all directions.

The additional degrees of freedom available to photoisomers bound to the pentacene and dodecene templates are responsible for a smaller increase in $\Delta E$ with respect to the gas phase compared to the same photoisomers bound to graphene or CNT templates. However, it is important to note that the template plays another role in determining the energetic properties of hybrids by sterically preventing rotation of the untethered phenyl ring. Thus, although there may be several possible cis isomers—for example, due to asymmetry in position or identity of functional groups, as in Fig. 3—the identity of the bound cis isomer is uniquely determined by the configuration of the minimum energy trans isomer. Upon photoexcitation, the ground state trans isomer converts to a specific cis configuration; in the example shown in Fig. 3, the molecule in this state stores $\Delta E$=1.27 eV/azo. In the gas phase, the molecule undergoes rapid thermal isomerization via ring rotation to a lower energy cis isomer, ultimately storing only 0.99 eV/azo. In closely packed phases, however, this ring rotation is sterically inhibited (the rotating ring would have to pass *through* neighboring molecules), trapping the higher energy cis isomer and storing more energy.

The trends discussed above suggest that increasing the ordering of the bound photoisomers should increase the energy storage capacity of the photoisomer/molecular template hybrids. One way to accomplish this is to increase the rigidity of the photoisomers. For example, the class II molecules are inherently stiffer than their class I analogues due to increased size and an additional planar phenyl ring. A useful measure of the deviation from the gas phase geometry is the C–N=N angle $\phi_{\text{C–N=N}}$ formed by the untethered phenyl ring in the templated molecules. In the gas phase, $\phi_{\text{C–N=N}}$ is 126° for both **1b** and **2b** molecules; in the more flexible **1b**/pentacene system $\phi_{\text{C–N=N}}$ is relatively unchanged (127°), whereas in the more rigid **2b**/pentacene system, it increases significantly to 137° as the steric interactions enforce a more narrow, elongated cis geometry.

Another approach to increase rigidity is to introduce bulky functional groups at the terminating carbons on the molecular templates. For example, $\beta$-carotene, the structure of which is essentially a polyalkene chain with bulky functional groups on both ends, enables a significant increase in $\Delta E$ compared to the pentacene and dodecene templates: Due to steric interactions between the end groups and the bound photoisomers, illustrated in Fig. 1, the photoisomers are constrained to a smaller volume, destabilizing the cis configuration and leading to a larger $\Delta E$.

Finally, one can also change the position of the linker moiety to increase the rigidity of a photoisomer/template hybrid, as indicated by the results for molecules **3a** and **3b**. Hybrids with these molecules are significantly less flexible, as deviation of the template-linker bond from the $sp^2$ geometry leads to unfavorable steric interactions between both the untethered phenyl groups and the template. As a result, they form more orderly arrays on the molecular templates. For example, this is illustrated by the atomic structure of the **3b**/pentacene system, shown in the supplementary material;[18] this system has a significantly larger $\Delta E$ than other photoisomer/molecular template systems, as well as good thermal stability and high $\eta_{\text{max}}$ (see Fig. 2). Furthermore, the attachment geometry minimizes the empty space in the hybrid structures, leading to a high volumetric energy density, as reported in Table I of the supplementary material.[18]

One can also significantly increase the thermal barrier, and thus the half-life of the metastable state, by taking advantage of intermolecular interactions in the templated systems. For example, hybrid structures including molecule **2c** (see, e.g., Fig. 4(c)), in which bulky dimethylamino groups are placed at the *para* positions of molecule **2b**, exhibit an approximately 25% increase in $E_a$ relative to **2b**. This increase, which arises due to unfavorable steric interactions between the dimethylamino substituents and the phenyl rings of closely packed neighbors in the transition state structure, leads to an enormous increase in the storage lifetime of the fuel (see Table II in the supplementary material[18]), a very useful characteristic for applications involving portable devices.

In addition to the thermal stability of the metastable state, another important property of a candidate solar thermal fuel is the temperature at which the stored heat is released when the isomerization of the metastable state is triggered (this can be done, e.g., via heat, a catalyst, application of an external voltage, or selective irradiation, depending on the chemistry of the fuel molecule, the geometry of the system, and the particular application). This temperature can be estimated as $T_{\text{release}} \approx \Delta E/C_p$, where $C_p$ is the heat capacity of the material; here this is estimated to be the same as that of solid azobenzene. As Fig. 2 shows, $T_{\text{release}}$ is predicted to be as high as ≈750 K for the photoisomer/template nanostructures considered in this study. Although these are only approximate estimates of Trelease, the significant improvement relative to non-templated azobenzene derivatives, as well as the inherent tunability of the system, suggests that it has the potential to provide a large temperature differential with which to do useful work.

The ability to achieve such high temperatures with nanostructured STFs raises questions about their thermal stability

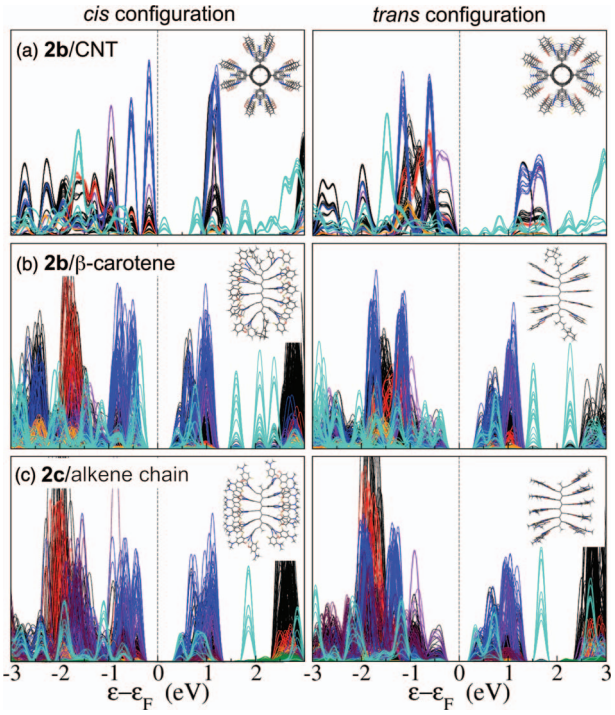


FIG. 4. Atom-projected DOS for the (a) **2b**/CNT, (b) **2b**/beta-carotene, and (c) **2c**/alkene chain systems. Black, blue, red, and orange curves represent the DOS of C, N, O, and F atoms, respectively; for clarity, the DOS corresponding to template C and amino N atoms are cyan and purple, respectively; in (c), the DOS of the C and N atoms on the dimethylamino groups are green and maroon, respectively.

with respect to desorption of the bound photoisomers. The computed photoisomer-template bond lengths for azobenzene molecules bound in an $sp^3$ geometry on CNTs, graphene, and $C_{60}$ are between 1.52 and 1.57 Å, similar to the bond length for a typical alkane C–C single bond (1.54 Å). For azobenzene molecules bound to molecular templates, such as dodecahendecaene, pentacene, and $\beta$-carotene, the photoisomer-template bond lengths are 1.46–1.50 Å, slightly larger than that of a typical alkene C=C double bond (1.34 Å). Thus, in all of the systems presented, the bond energies will be similar to or greater than 3.59 eV, the bond energy of a C–C single bond in an alkane. Given that thermal cracking of alkanes requires temperatures of $>$1000 K without the presence of a catalyst, and the highest values of $T_{\text{release}}$ are $<$800 K, it is unlikely that the photoisomers will "desorb" from the templates.

It is also important to note another advantage conferred by the thermophysical properties of the photoisomer/template hybrids: As their molecular weight is significantly larger than that of the non-bound photoisomers, the hybrids are much less volatile and, therefore, will not vaporize until $T \gg T_{\text{release}}$. This is extremely important in terms of applications: one does not want the fuel to undergo a transition to the gas phase upon triggering in a confined volume, as such behavior does not lend itself to high cyclability or safety.

In addition to modulating the energetic and thermal properties of the bound photoisomers, the templates have a significant effect on the electronic and optical properties. First, the template induces the formation of electronic bands due to the overlap of the molecular orbitals on neighboring azobenzenes. Second, in the molecular template systems, the template introduces a number of chemically distinct environments, thereby smearing the HOMO and LUMO peaks. For example, compared to the more orderly **2b**/CNT nanostructure (Fig. 4(a)), which exhibits single peaks similar to those found for gas phase **2b**, the HOMO and LUMO states of the **2b**/$\beta$-carotene system (Fig. 4(b)) are distributed over a range of energies, which could lead to a more gradual absorption onset. (This may also affect the extinction coefficient, but exploring this relationship is beyond the scope of the current study and will be examined in the future.) Finally, the template can shift the HOMO and LUMO energies of the bound photoisomers, modifying the overlap between the absorption spectrum and the solar spectrum and changing the external efficiency,

$$\eta = f_{\text{converted}} f_{\text{absorbed}} = -\Delta E \int_0^{\lambda_{\max}} \frac{h}{c} \frac{d\lambda}{\lambda^2} \frac{\int_0^{\lambda_{\max}} I(\lambda) d\lambda}{\int_0^{\infty} I(\lambda) d\lambda},$$

where $I(\lambda)$ is the solar flux. The computed values of the HOMO-LUMO gap $E_{\text{gap}}$, $\lambda_{\max}$, and the maximum theoretical efficiency $\eta_{\max}$ are reported in the supplementary material.[18] We note that the estimate of $\eta_{\max}$ assumes that (a) there exists an excited state that enables trans-to-cis isomerization and (b) this state is near the LUMO of the bound photoisomers. These are reasonable assumptions because (a) in all of the systems, the LUMO states or states with energy near the LUMO have similar character to the LUMO of gas phase azobenzene (i.e., they are primarily localized on the azo group), which is responsible for the isomerization, and (b) the photoisomerization of numerous azobenzene derivatives has been well documented and is observed to occur upon illumination with photons at visible and UV frequencies.

In general, the hybrid nanostructures are predicted to achieve higher external efficiencies than isolated azobenzene derivatives, for which $1<\eta_{\max}<5\%$, as illustrated in Fig. 2. This trend is partially attributed to a redshift in $\lambda_{\max}$, similar to that observed in *J*-aggregates,[20] that arises from coupling between the dipoles of neighboring close-packed molecules. However, as Fig. 2 shows, when the photoisomers are bound to the template via C–C single bonds (i.e., the template carbon involved in the bond is $sp^3$), the maximum efficiency is still relatively low ($6<\eta_{\max}<13\%$ for CNT, graphene, and fullerene templates. In contrast, when the photoisomers are bound to the template via C=C double bonds, as with the pentacene, dodecene, and $\beta$-carotene templates, the maximum efficiency is significantly higher, with $\eta_{\max}>20\%$ in most systems and as high as 35% for the **2c**/dodecene system (indicated by the large orange triangle in Fig. 2).

In these systems, the $\pi - \pi$ conjugation is extended over the entire photoisomer/template supermolecule and strong hybridization occurs between the HOMO (LUMO) of the template and the HOMO (LUMO) of the bound photoisomers, leading to a significant decrease in $E_{\text{gap}}$ with respect to the isolated photoisomers. The atom-projected density of states (DOS) in Fig. 4(c) illustrates this behavior for the **2c**/dodecene hybrid. Replacing the molecular template with a CNT, graphene, or fullerene template, in which the $sp^3$ geometry of the attachment sites prevents continuous conjugation over the entire system reopens the HOMO-LUMO gap,

as shown by comparison of the DOS of the **2b**/CNT and **2b**/$\beta$-carotene systems in Figs. 4(a) and 4(b), respectively.

The maximum efficiency is constrained by the fact that an absorbed photon must have energy greater than $\Delta E$ to enable a transition from the ground to the metastable state. The lowest energy photon that can be absorbed by a photoisomer is thus $hc/\lambda_{max} = E_{gap} = \Delta E + \Delta_{min}$, where $\Delta_{min}$ is simply the energy difference between the LUMO of the ground state and the HOMO of the metastable state (see Fig. 2). Depending on the energy level of the lowest excited state PES that leads to photoisomerization, $\eta_{max}$ can approach 50%, significantly above the Shockley-Queisser limit[21] for single junction solar cells (33.7%), as well as current photocatalytic water splitting schemes (≈10%–12%; see, e.g., Refs. 22 and 23). The high theoretical efficiency is due to the fact that, unlike the other two technologies, the efficiency of STFs is not limited by recombination, instead governed only by blackbody radiation and solar spectrum losses. Of course, unlike solar cells and photocatalytic water splitting, which can convert sunlight directly to electricity, STFs convert sunlight to high temperature heat; if one wishes to then convert the output heat to electricity, the efficiency takes another hit. Nevertheless, assuming an efficiency of around 30% for the heat-to-electricity conversion process, one could achieve, in principle, 15% efficiency for the net solar-to-electricity conversion with solar thermal fuels.

It is also important to note that, unlike the situation with solar cells, the efficiency of a STF is not necessarily a critical metric. For example, in designing a fuel to power a solar cooker that captures and stores solar energy during the day for use at night, it would be reasonable to sacrifice external efficiency for a higher $\Delta E$ and thus a higher energy density, as the latter governs practical issues such as the length of time for which one can use the fuel to boil water. As long as $\eta_{max}$ is sufficiently high that all of the fuel is "charged" over the course of a day (i.e., enough photons are absorbed to convert every molecule into the metastable state), increasing $\eta_{max}$ will not enable one to store additional energy and thus does not need further optimization. Increasing $\eta_{max}$ will, however, enable the same amount of fuel to be charged more quickly, or more fuel to be charged over the same time period given a fixed spatial footprint. These capabilities may be important, for example, in designing a STF to power a steam turbine and generate electricity. For this application, the fuel would need to be cycled many times over the course of the day to provide a continuous supply of heat, and the power output will be limited by the charging time. Therefore, an important design goal would be to optimize $\eta_{max}$ in order to minimize the time and/or footprint required to charge a large amount of the STF. Other contributions to the total efficiency, such as the absorption depth of the fuel, and any effects due to the reactivity of the excited state with other molecules in the environment will also affect the charging time and efficiency. These issues, likely best addressed at the device design level, will be examined in future work.

In conclusion, we have used density functional theory to demonstrate the promising capabilities of the photoisomer/template platform as a customizable solar energy storage and conversion technology. We have shown that key macroscopic properties—energy density, thermal stability, absorption efficiency—can be tuned via atomic-scale engineering of structural and electronic properties through the use of a template, and we have provided general guidelines for choosing the template material in order to optimize specific STF properties, thereby potentially enabling a wide range of applications. In addition, we have designed a specific set of promising azo/carbon-based template systems that are predicted to have energy densities in the range of Li-ion batteries, tunable thermal stability from minutes to years, and potential external efficiencies of up to 35%. Furthermore, we have shown that the theoretical maximum efficiency can be as high as 50% for the general class of solar thermal fuels. With a large range of the photoisomer/template phase space yet to be explored, there are numerous exciting possibilities for further property enhancement and customization, suggesting that solar thermal fuels could become a competitive renewable energy technology.

The authors acknowledge financial support from ARPA-E as well as computational support from LLNL, NERSC, and Teragrid.

[1] C. Phillippopoulos, D. Economou, C. Economou, and J. Marangozis, Ind. Eng. Chem. Prod. Res. Dev. **22**, 627 (1983).
[2] A. D. Dubonosov, V. A. Bren, and V. A. Chernoivanov, Russ. Chem. Rev. **71**, 917 (2002).
[3] R. Boese, J. K. Cammack, A. J. Matzger, K. Pflug, W. B. Tolman, K. P. C. Vollhardt, and T. W. Weidman, J. Am. Chem. Soc. **119**, 6757 (1997).
[4] Y. Kanai, V. Srinavasan, S. K. Meier, K. P. C. Vollhardt, and J. C. Grossman, Angew. Chem. **49**, 8926 (2010).
[5] K. Moth-Poulsen, D. Coso, K. Börjesson, N. Vinokurov, S. K. Meier, A. Majumdar, K. P. C. Vollhardt, and R. A. Segalman, Energy Environ. Sci. **5**, 8534 (2012).
[6] S. J. van der Molen and P. Liljeroth, J. Phys.: Condens. Matter **22**, 133001 (2010).
[7] M.-M. Russew and S. Hecht, Adv. Mater. **22**, 3348 (2010).
[8] V. Balzani, A. Credi, and M. Venturi, Chem. Soc. Rev. **38**, 1542 (2009).
[9] E. R. Kay, D. A. Leigh, and F. Zerbetto, Angew. Chem., Int. Ed. **46**, 72 (2007).
[10] *Smart Light-Responsive Materials Azobenzene-Containing Polymers and Liquid Crystals*, edited by Y. Zhao and T. Ikeda (Wiley, Hoboken, NJ, 2009).
[11] M. Alemani, S. Selvanathan, F. Ample, M. V. Peters, K.-H. Rieder, F. Moresco, C. Joachim, S. Hecht, and L. Grill, J. Phys. Chem. C **112**, 10509 (2008).
[12] Y. Feng, W. Feng, H. Noda, A. Fujii, M. Ozaki, and K. Yoshino, J. Appl. Phys. **102**, 053102 (2007).
[13] J. M. Simmons, I. In, V. E. Campbell, T. J. Mark, F. Leonard, P. Gopalan, and M. A. Eriksson, Phys. Rev. Lett. **98**, 086802 (2007).
[14] H. Taoda, K. Hayakawa, K. Kawase, and H. Yamakita, J. Chem. Eng. Jpn. **20**, 265 (1987).
[15] J. Olmsted III, J. Lawrence, and G. G. Yee, Sol. Energy **30**, 271 (1983).
[16] T. Nagai, K. Fujii, I. Takahashi, and M. Shimada, Bull. Chem. Soc. Jpn. **74**, 1673 (2001).
[17] A. A. Blevins and G. J. Blanchard, J. Phys. Chem. B **108**, 4962 (2004).
[18] See supplementary material at http://dx.doi.org/10.1063/1.4773306 for detailed methods and values for all computed properties.
[19] A. M. Kolpak and J. C. Grossman, Nano Lett. **11**, 3156 (2011).
[20] A. Eisfeld and J. S. Briggs, Chem. Phys. **324**, 376 (2006).
[21] W. Shockley and H. J. Queisser, J. Appl. Phys. **32**, 510 (1961).
[22] S. K. Pilli, T. E. Furtak, L. D. Brown, T. G. Deutsch, J. A. Turner, and A. M. Herring, Energy Environ. Sci. **4**, 5028 (2011).
[23] Y. Hou, B. L. Abrams, P. C. K. Vesborg, M. E. Bjorketun, K. Herbst, L. Bech, A. M. Setti, C. D. Damsgaard, T. Pedersen, O. Hansen *et al.*, Nature Mater. **10**, 434 (2011).